Electronic Seismologist

GITpy: A Python Implementation of the Generalized Inversion Technique

Paola Morasca*[1], Maria D'Amico[2], Daniele Spallarossa[3], Dino Bindi[4], Matteo Picozzi[5], Adrien Oth[6], and Francesca Pacor[1]

Abstract

GITpy is an open-source object-oriented Python software package implementing the well-established Generalized Inversion Technique (GIT), a spectral decomposition approach to isolate the source, propagation, and site contributions from *S*-phase Fourier amplitude spectra (FAS) (Andrews, 1986; Castro *et al.*, 1990; Boatwright *et al.*, 1991; Drouet *et al.*, 2008; Edwards *et al.*, 2008; Oth *et al.*, 2011; Bindi *et al.*, 2020). GITpy applies a nonparametric (i.e., without imposing any a priori parametric models on the different terms), one-step inversion procedure. GITpy offers the possibility to: (1) simplify the attenuation and source modeling process by providing configuration files and interactive procedures allowing for rapid testing of different models; (2) choose between different levels of attenuation modeling complexity (geometrical spreading and anelastic attenuation); (3) select among different source spectrum modeling options, including the use of a homogeneous or heterogeneous crustal model, as well as the ability to define the frequency range for the model fitting; (4) calculate station-specific apparent source spectra by correcting the input FAS for site amplification and nonparametric attenuation obtained from the inversion, and then fit them. This can be particularly useful for directivity studies. Furthermore, this module can be used independently for a rapid estimation of source parameters in case of a strong event; (5) provide several source parameters including radiated energy, apparent stress, and radiation efficiency alongside seismic moment, corner frequency, and stress drop. Here, we present the versatility of GITpy by applying it to the well-documented 2016–2017 seismic sequence in central Italy, showcasing the software's capabilities through specific modules for source and attenuation modeling, as well as for calculating apparent source spectra. To achieve this, a comprehensive dataset including 355 stations and 8534 events was assembled, allowing for the evaluation of the software's performance in handling large-scale datasets.

Cite this article as Morasca, P., M. D'Amico, D. Spallarossa, D. Bindi, M. Picozzi, A. Oth, and F. Pacor (2025). GITpy: A Python Implementation of the Generalized Inversion Technique, *Seismol. Res. Lett.* **96**, 3866–3879, doi: 10.1785/0220250042.

Supplemental Material

Introduction

The Generalized Inversion Technique (GIT) was developed in the 1980s through key studies like Andrews (1986), Castro *et al.* (1990), and Boatwright *et al.* (1991), and has been refined in recent years (Oth *et al.*, 2011; Bindi and Kotha, 2020; Grendas *et al.*, 2021). Different inversion strategies have been proposed, including parametric (Drouet *et al.*, 2008, 2010; Edwards *et al.*, 2008; Zollo *et al.*, 2014; Grendas *et al.*, 2021) and nonparametric (Andrews, 1986; Castro *et al.*, 1990; Oth *et al.*, 2011; Bindi *et al.*, 2020) approaches, each with strengths and weaknesses based on the application and data availability (Shible *et al.*, 2022).

The parametric approach assumes a known attenuation function, simplifying the inversion by reducing the number of parameters. This is suitable for regions with well-defined

1. Istituto Nazionale di Geofisica e Vulcanologia, INGV, Milan, Italy, https://orcid.org/0000-0002-6525-4867 (PM); https://orcid.org/0000-0001-5745-0414 (FP); 2. Istituto Nazionale di Geofisica e Vulcanologia, INGV, Catania, Italy, https://orcid.org/0000-0002-1677-1294 (MDA); 3. Dipartimento di Scienze della Terra dell'Ambiente e della Vita, University of Genoa, Genoa, Italy, https://orcid.org/0000-0002-8021-3908 (DS); 4. German Research Centre for Geosciences, GFZ, Potsdam, Germany, https://orcid.org/0000-0002-8619-2220 (DB); 5. National Institute of Oceanography and Applied Geophysics, OGS, Udine, Italy, https://orcid.org/0000-0001-8078-9416 (MP); 6. European Center for Geodynamics and Seismology, ECGS, Walferdange, Luxembourg, https://orcid.org/0000-0003-4859-6504 (AO)

*Corresponding author: paola.morasca@ingv.it

geological settings but less effective in complex areas. For example, in Italy, this method was applied in the northeast by Cataldi *et al.* (2023) and for microearthquakes in Irpinia by Zollo *et al.* (2014).

The nonparametric approach is data-driven and allows model-free reconstruction of earthquake source, attenuation, and site functions. Although fewer assumptions are made, it requires large datasets for robust models. The increasing availability of high-quality data from modern networks makes this approach ideal for studying larger regions. This method can be applied either as a one-step scheme (Oth *et al.*, 2011) or a two-step scheme (Castro *et al.*, 1990; Bindi *et al.*, 2009). In a two-step approach, attenuation is first solved, followed by the separation of source and site terms using attenuation-corrected Fourier amplitude spectra (FAS). Wang *et al.* (2019) applied a two-step approach to analyze the Amatrice–Norcia–Visso seismic sequence (2016–2017), observing breakdown in self-similarity. Bindi *et al.* (2024) used the two-step method for seismic data in central/southern Italy, highlighting variations in seismic moment and corner frequency.

The one-step approach was used by Oth *et al.* (2011) to analyze data from Japan's Kyoshin and Kiban–Kyoshin seismic networks. This method has since been applied in various regions with several data, including Italy (Ameri *et al.*, 2011; Pacor, Spallarossa, *et al.*, 2016; Bindi *et al.*, 2020; Picozzi *et al.*, 2021; Morasca *et al.*, 2022, 2023) and other areas such as Türkiye (Bindi, Zaccarelli, Cotton, *et al.*, 2023), New Zealand (Oth and Kaiser, 2014; Zhu *et al.*, 2024), and Ridgecrest (Bindi *et al.*, 2021).

Choosing the optimal inversion strategy depends on dataset characteristics and amount of data (Shible *et al.*, 2022), with processing and modeling assumptions also influencing results (Bindi *et al.*, 2023a,b). Although GIT is widely used, most researchers rely on home-made software, some of which is publicly available, like GITANES (Klin *et al.*, 2018), developed in MATLAB. The software from Oth *et al.* (2011) includes post-inversion modeling, while Klin's focuses on site amplification.

This study introduces the open-source software package GITpy, which implements the non-parametric one-step approach in Python with an object-oriented structure. This allows future feature additions and improvements, making the code more accessible and up-to-date. GITpy is a key tool for seismic monitoring, hazard assessment, and earthquake engineering. The software's functionality is demonstrated using a large dataset for central Italy, a region previously studied with GIT (Pacor, Spallarossa, *et al.*, 2016; Morasca *et al.*, 2023; Bindi *et al.*, 2024), providing a basis for comparison and performance validation.

Dataset

To demonstrate GITpy's potential, we built a comprehensive dataset (CI_db) for central Italy, including 355 stations and 8534 events (M_L 1.8–6.2), with ~400,000 recordings per frequency (Fig. 1). GITpy can efficiently handle large datasets and produce results quickly, depending on machine performance (detailed in the supplemental material, available to this article). This is crucial for researchers running multiple tests to explore assumptions before finalizing the analysis. As outlined by Bindi, Spallarossa, *et al.* (2023), GIT solutions are non-unique due to two undetermined degrees of freedom, requiring careful assumption settings tailored to the dataset (Shible *et al.*, 2022; Bindi, Spallarossa, *et al.*, 2023). This necessitates multiple inversions to optimize the GIT scheme.

The CI_db consists of three-component accelerometric and velocimetric recordings from temporary and permanent networks by the National Institute of Geophysics and Volcanology (INGV) and by the Italian Department of Civil Protection (DPC) (see Data and Resources), spanning 2015–2018 including the 2016–2017 Amatrice–Norcia–Visso seismic sequence (Tinti *et al.*, 2016; Chiaraluce *et al.*, 2022). The dataset offers dense spatial sampling (Fig. 1a), hypocentral distances of 5–150 km (80% within 50 km, Fig. 1d), and a mean earthquake depth of 10 km (Fig. 1c). Recordings were corrected for instrumental response, converted to acceleration. FAS are calculated on the vectorial composition of the two horizontal components in the 0.2–40 Hz range. *S*-wave windows were selected based on cumulated energy percentages and event-station distances (i.e., 5%–90% for <25 km, 5%–80% for 25–50 km, 5%–70% for >50 km).

Signal-to-noise ratios were calculated, applying a threshold of 3.5, and spectral amplitudes were smoothed with the Konno and Ohmachi (1998) algorithm (b = 40). Events with fewer than 10 stations, stations with fewer than 10 events, distances larger than 125 km, and frequencies below 0.5 Hz or above 25 Hz were excluded for quality assurance. The lowest sampled frequency is 0.59 Hz (350,698 records), while the most sampled frequency is 5.94 Hz (406,866 records).

Method

GIT separates source, propagation, and site contributions from the FAS of recorded *S* waves. After inversion, nonparametric attenuation and source functions can be fitted with standard seismological models to derive seismic parameters (e.g., seismic moment, corner frequency, stress drop, quality factor, κ operator, and geometrical spreading). Post-inversion fitting ensures that chosen models for one term do not affect results for other terms, allowing multiple parametric models to be tested without repeated inversions.

GITpy includes four modules: GITeps.py for generalized *S*-wave FAS inversion, CorrectFas.py for calculating apparent source spectra, FitSource.py for modeling source terms, and FitAttenuation.py for modeling attenuation terms. A flowchart of GITpy is shown in Figure 2. To install and run GITpy, users can follow instructions in the GitLab repository readme (see Data and Resources; D'Amico *et al.*, 2025). Required Python libraries must also be installed. Modules are run via the command line with configuration and log files written in

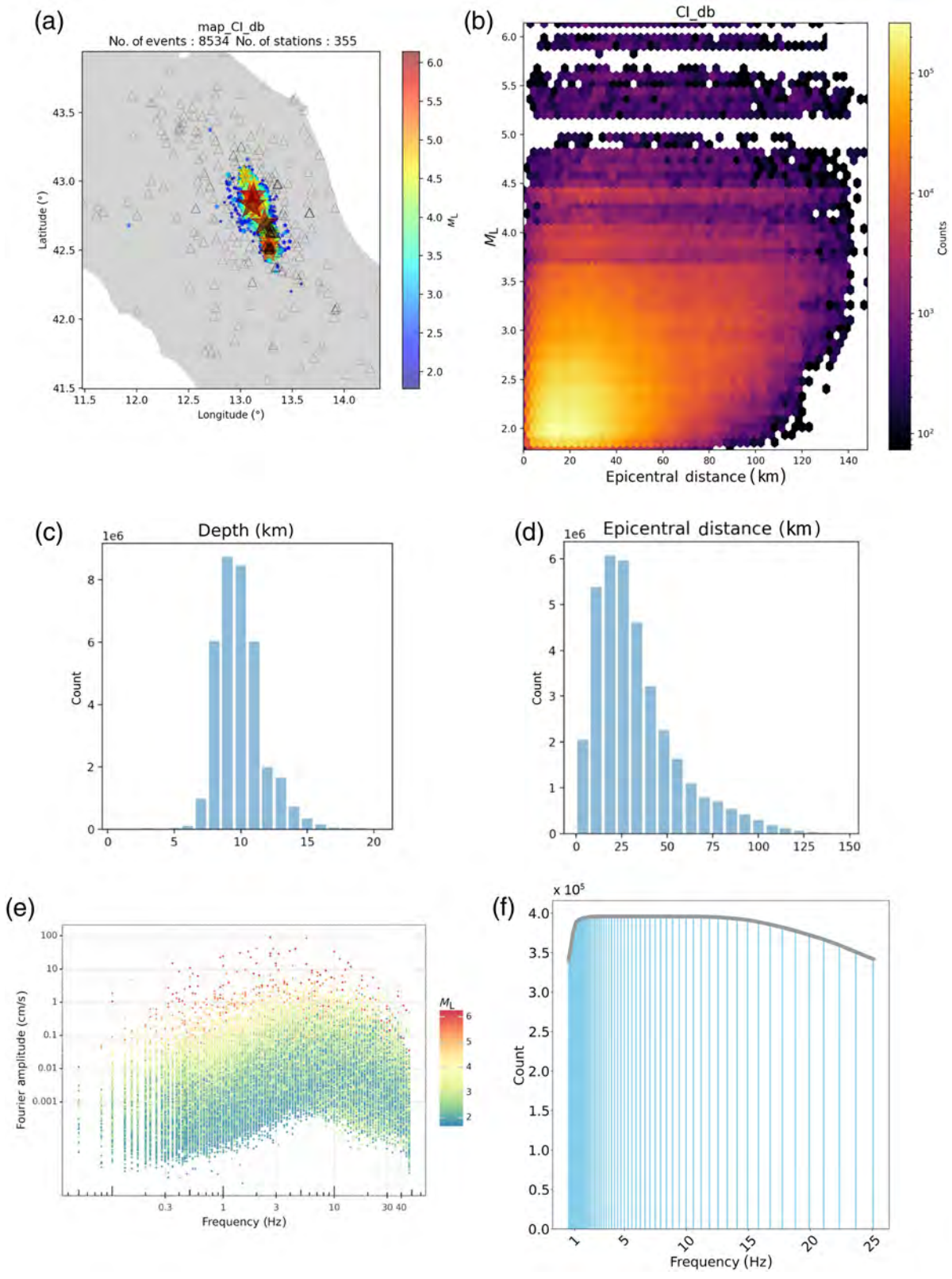

Figure 1. Dataset of Fourier amplitude spectra (FAS) used for central Italy Generalized Inversion Technique (GIT) compiled for this study (CI_db); (a) spatial distribution of seismic events colored by magnitude (M_L) and stations (triangles); (b) magnitude–distance distribution with recording counts; (c) earthquake depth histogram; (d) epicentral distance histogram; (e) FAS of the horizontal ground acceleration components (vectorial composition); and (f) number of postprocessed records for each frequency band. The color version of this figure is available only in the electronic edition.

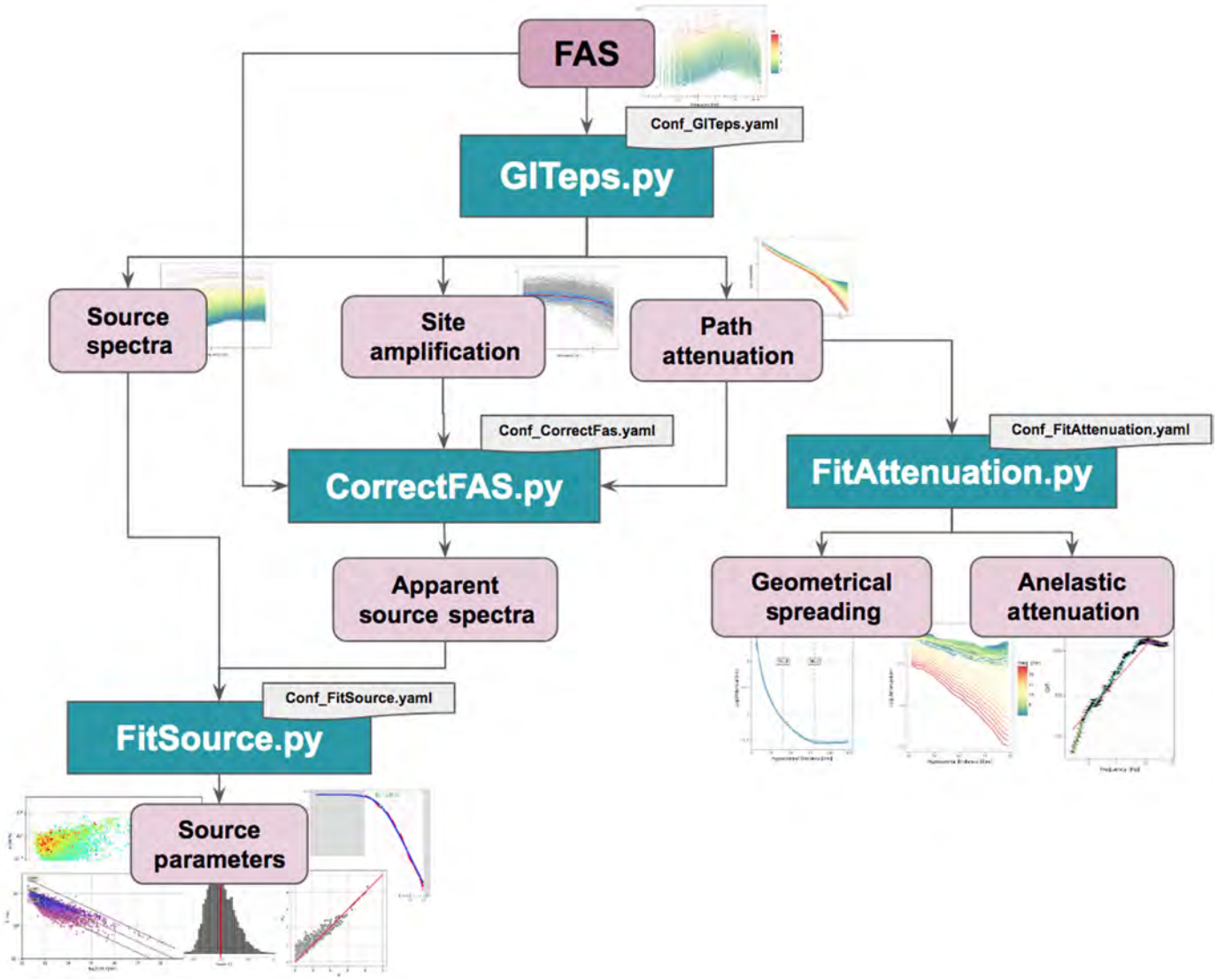

Figure 2. Flowchart of GITpy. The color version of this figure is available only in the electronic edition.

human-readable YAML format. Examples of module usage are provided in the repository (see Data and Resources).

GITeps.py: Generalized inversion technique

GITeps.py implements a nonparametric inversion approach based on the convolutional assumption that the FAS of earthquake i recorded at station j is the product of source (S), propagation (P), and site (Z) contributions:

$$\mathrm{FAS}_{ij}(R_{ij},f) = S_i(f) \times P(R_{ij},f) \times Z_j(f), \quad (1)$$

in which R_{ij} is the hypocentral distance and f is the frequency. Analyzing each frequency separately, this equation generates an overdetermined linear system that can be solved via least squares. However, two unresolved degrees of freedom make the solution nonunique. To address this, two a priori constraints are applied: (1) setting the average logarithm of all site amplifications, or those of reference bedrock stations, to a fixed value, usually zero, and (2) fixing the attenuation term's logarithm to zero at a reference distance, regardless of frequency. The effects of different assumptions are discussed in Bindi, Spallarossa, *et al.* (2023).

Running GITeps.py is essential for the GITpy workflow (Fig. 2). Optional settings allow users to import files with distance bins for inversion or exclude specific seismic events and stations from the dataset.

CorrectFas.py: Apparent source spectra calculation

The module CorrectFas.py (Fig. 2) adjusts recorded FAS for attenuation and site effects derived from GITeps.py, providing station-specific estimates of near-source Fourier spectra, termed "apparent source spectra". These spectra, recorded for a single earthquake at each station, can be input into the FitSource.py module to analyze ground-motion variability by azimuth and distance (Fig. 2). Comparing the apparent source spectra of a single earthquake with the mean source

spectrum can help identify directivity effects and rupture complexity (Pacor, Gallovič, *et al.*, 2016). This module is also useful for quickly estimating source parameters for new events.

FitSource.py: Source spectra parameterization

The FitSource.py module (Fig. 2) models earthquake spectra using standard seismological models, providing various source parameters (i.e., seismic moment, corner frequency, stress drop, radiated energy, ratio between observed and full energy, apparent stress, and radiation efficiency). It processes both mean source spectra from GITeps.py and apparent source spectra from CorrectFas.py, using a standardized ".source" format. The configuration file defines inputs, outputs, and parameters required to constrain the ω^2 model (e.g., crustal medium properties, reference distance, and radiation pattern), the kappa source (κ_s), and the lower frequency bound (f_h) used for estimating κ_s. Optional files can constrain seismic moment using reference catalogs, define magnitude-dependent frequency ranges, or incorporate a 1D crustal model.

In the current version of GITpy, only the ω^2 model (Brune, 1970, 1971) has been implemented (equation 2) to fit the GIT derived nonparametric source spectra:

$$S(f) = \frac{R_{\theta\phi}A}{4\pi\varrho\beta^3 R_0} M_0 (2\pi f)^2 \frac{1}{1+\left(\frac{f}{f_c}\right)^2} e^{-\pi\kappa_s(f-f_h)}, \tag{2}$$

in which $R_{\theta\phi}$ represents the average *S*-wave radiation pattern commonly set to 0.55; the constant parameter A accounts for the free-surface amplification factor, usually assumed equal to 2, ρ and β are the assumed density [g/cm^3] and the *S*-wave velocity [km s^{-1}] for the study region, R_0 indicates the reference distance [km], which is usually set to the lowest or best sampled distance bin.

FitSource.py simultaneously fits the seismic moment M_0 [N · m] and the corner frequency f_c [Hz]. As a first step, the acceleration source spectrum is corrected only above the hinge frequency f_h to remove the kappa effects. Then, in the second step, the displacement source spectrum is fitted by Brune's model. Because FitSource.py adopts a linearized inversion, the starting model is provided by initially setting M_0 and f_c around theoretical values defined by equations (3) (Kanamori, 1977) and (4) (Brune, 1970, 1971), respectively:

$$M_0 = 10^{1.5\times M_w + 9.1}, \tag{3}$$

$$f_c = 4.9\times 10^6 \times \beta \sqrt[3]{\frac{\Delta\sigma}{M_0}}. \tag{4}$$

M_0 in equations (3) and (4) is in Newton meter, whereas $\Delta\sigma$ is fixed to 3 MPa.

Fitting the source terms for large datasets of seismic events, ranging from small to large magnitudes and recorded in regions with heterogeneous crustal properties, is a challenging task. For instance, limited bandwidth at low frequencies often prevents the observation of the corner frequencies in the source spectra of large earthquakes ($M_w > 5.5$). To address this issue, we implemented in FitSource.py the possibility to constrain the seismic moment of large events using M_w estimates from independent resources. In this scenario, the corner frequency (f_c) becomes the sole free parameter to be fitted in equation (2).

Once M_0 and f_c are obtained for each earthquake, the Brune stress drop is calculated as follows:

$$\Delta\sigma = \frac{7M_0}{16r^3}, \tag{5}$$

in which r is the source radius of a circular fault model (Brune, 1970, 1971):

$$r = \frac{2.34\beta}{2\pi f_c}. \tag{6}$$

The apparent stress τ_a [N/m^2], which provides a measure of how efficiently an earthquake radiates energy, is calculated as defined by Wyss (1970):

$$\tau_a = \mu\frac{E_s}{M_0}, \tag{7}$$

in which μ [N/m^2] is the shear modulus of rigidity of the source material and E_s [J] is the seismic energy radiated from the source.

By ignoring the contribution from *P* waves, which accounts for ~5% of the total radiated energy (Aki and Richards, 2002), in FitSource.py, we assess seismic energy E_S from both theoretical and observed spectra. In the first case, the seismic moment and corner frequency derived from GIT are used in equation (8) (Izutani and Kanamori, 2001), with the integration performed up to ten times the corner frequency of each earthquake:

$$E_S = \frac{4\pi}{5\varrho\beta^5}\int_0^{+\infty}\left|\frac{M_0 f}{1+\left(\frac{f}{f_c}\right)^2}\right|^2 df. \tag{8}$$

In the second case, the radiated energy is estimated by equation (9):

$$E_S = \frac{16\pi\varrho\beta R_0^2}{5A^2(R^{\theta\phi})^2}\int_{f_{\min}}^{f_{\max}} |S_{\mathrm{vel}}|^2 df, \tag{9}$$

in which S_{vel} is the empirical velocity source spectrum at the reference distance R_0.

However, because the empirical source spectra provided by GIT are defined over a finite-frequency range [$f_{\min} - f_{\max}$], the energy estimation may be affected by this inherent bandwidth

limitation (Ide and Beroza, 2001). Given that over 80% of the seismic energy could be radiated at frequencies exceeding the corner frequency, a finite bandwidth correction was applied to equation (9) to account for the energy radiated up to infinite frequency, as expressed in equation (10):

$$\int_{f_{\min}}^{f_{\max}} |S_{\mathrm{vel}}|^2 df = \kappa v \int_{-\infty}^{\infty} |S_{\mathrm{vel}}|^2 df. \tag{10}$$

The ratio between observed and total energy (Ide and Beroza, 2001; Wang, 2004) is reported in equation (11):

$$kv = \frac{2}{\pi}\left[-\frac{\left(\frac{f_{\max}}{f_c}\right)}{1+\left(\frac{f_{\max}}{f_c}\right)^2} + \frac{\left(\frac{f_{\min}}{f_c}\right)}{1+\left(\frac{f_{\min}}{f_c}\right)^2} + \tan^{-1}\frac{f_{\max}}{f_c} - \tan^{-1}\frac{f_{\min}}{f_c} \right]. \tag{11}$$

Finally, the radiation efficiency η_{sw} is computed as the ratio between the apparent stress τ_a and static stress drop $\Delta\sigma$ (Savage and Wood, 1971; Beeler *et al.*, 2003; 2012):

$$\eta_{sw} = \frac{\tau_a}{\Delta\sigma}. \tag{12}$$

FitAttenuation.py: Parameterization of the seismic wave path attenuation

FitAttenuation.py (Fig. 2) performs parametric regression of GIT-derived attenuation curves using standard seismological models for geometrical spreading, anelastic attenuation, and high-frequency decay (equation 13). Geometrical spreading $G(R)$ can be modeled as a piecewise function of hypocentral distance R (equation 14 and for parameters description, see Table S1) by fitting the mean amplitude of nonparametric attenuation curves around 1 Hz (Pacor, Spallarossa, *et al.*, 2016). Users can define up to three hinge distances, whereas model exponents are derived via linear regression. Anelastic attenuation is characterized by the frequency-dependent quality factor $Q(f) = Q_0 f^N$ for which evaluation depends on the accuracy of the geometrical spreading model due to their interdependence. High-frequency decay beyond the hinge frequency f_h (consistent with the value used in equation 2) is modeled using the k_r parameter (Anderson and Hough, 1984),

$$\ln[P(R_{ij}f)] = \ln[G(R)] - \frac{\pi f(R-R_0)}{Q(f)\beta} - \pi k_r(f - f_h), \tag{13}$$

$$G(R) = \begin{cases} \left(\frac{R_0}{R}\right)^{n1} & \text{for } R \le HD_1 \\ \left(\frac{R_0}{HD_1}\right)^{n1}\left(\frac{HD_1}{R}\right)^{n2} & \text{for } HD_1 < R \le HD_2 \\ \left(\frac{R_0}{HD_1}\right)^{n1}\left(\frac{HD_1}{HD_2}\right)^{n2}\left(\frac{HD_2}{R}\right)^{n3} & \text{for } HD_2 < R \le HD_3 \\ \left(\frac{R_0}{HD_1}\right)^{n1}\left(\frac{HD_1}{HD_2}\right)^{n2}\left(\frac{HD_2}{HD_3}\right)^{n3}\left(\frac{HD_3}{R}\right)^{n4} & \text{for } R > HD_3 \end{cases}. \tag{14}$$

Typically, $G(R)$ is assumed frequency-independent (Bindi and Kotha, 2020; Morasca *et al.*, 2022; Bindi *et al.*, 2024), though frequency-dependent models may be more appropriate in some cases. FitAttenuation.py allows testing frequency-dependent geometrical spreading across user-defined frequency ranges.

Once the geometrical spreading is calibrated, it is applied to correct the nonparametric attenuation to isolate the contributions of anelastic attenuation. Specifically, a preliminary fit of the $G(R)$-corrected attenuation (in natural logarithm) is performed using a user-defined hinge frequency f_h, incorporating the linear term $-\pi k_r(f-f_h)$. This step removes the k_r from the $G(R)$-corrected attenuation curves, leaving the residual attenuation to represent solely the anelastic attenuation component (equation 15):

$$\ln[P(R,f)]_{\mathrm{corr}} = C(R-R_0) = \frac{-\pi f(R-R_0)}{Q(f)\beta}. \tag{15}$$

Subsequently, a least-squares regression is performed over a selected distance range in which the $G(R)$ and κ-corrected attenuation curves exhibit linear trends. This regression is used to derive a frequency-dependent quality factor $Q(f)$, which characterizes the anelastic attenuation. $Q(f)$ can be modeled either as a monotonically increasing function of frequency $Q(f) = \frac{-\pi f}{C\beta} = Q_0 f^N$ reflecting a simple dependence on frequency, or as a trilinear function with user-defined hinge frequencies (HF_1 and HF_2) (equation 16), allowing for a more flexible representation of the frequency-dependent behavior of attenuation:

$$Q(f) = \begin{cases} Q_{01} f^{N1} & \text{for } f \le \mathrm{HF}_1 \\ Q_{02} f^{N2} & \text{for } \mathrm{HF}_1 < f < \mathrm{HF}_2 \\ Q_{03} f^{N3} & \text{for } f \ge \mathrm{HF}_2 \end{cases}. \tag{16}$$

However, a limitation of this procedure is that the nonparametric curves corrected for the geometrical spreading near 1 Hz (equation 15) tend to maintain zero amplitude across the entire distance range. Therefore, the corresponding quality factors approach infinity around 1 Hz, and the $Q(f)$ trend deviates significantly from linearity. Examples of nonparametric curves with $k_r = 0$ and corrections for $G(R)$ are provided in the supplemental material of this study (see model AT1 in Fig. S2). To address this issue, one approach is to balance the trade-off between geometrical spreading and anelastic attenuation by also correcting the nonparametric attenuation for anelastic effects around 1 Hz (Bindi and Kotha, 2020; Bindi, Zaccarelli, Razafindrakoto, 2023). This adjustment can be managed in FitAttenuation.py by setting corr_fact_flag = 1 and Q0_corr equal to the assumed quality factor at 1 Hz in the configuration file. Examples of nonparametric curves with $k_r = 0$, corrected for both $G(R)$ and anelastic attenuation at 1 Hz, are included in the supplemental material of this study (see models AT2–AT4 in Fig. S2).

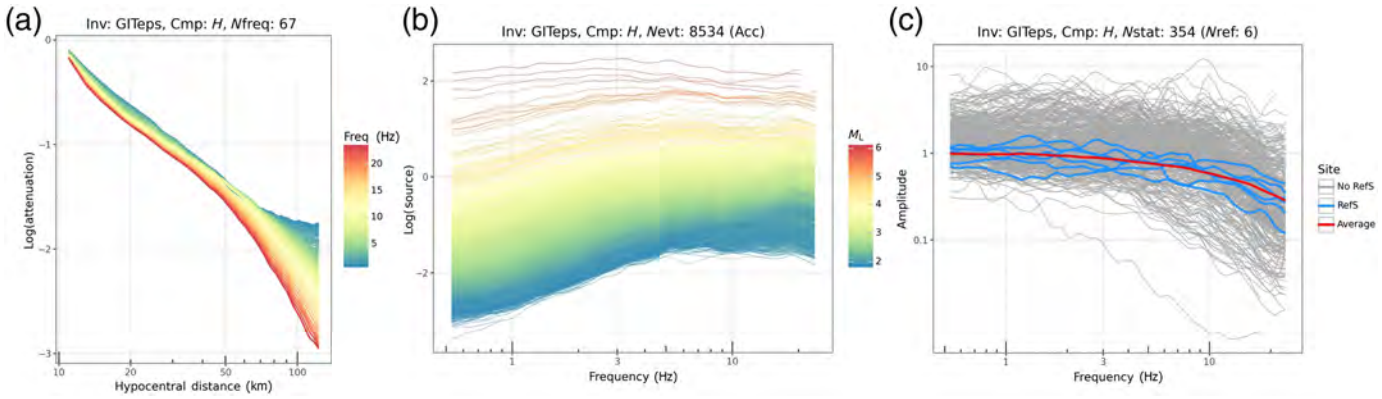

Figure 3. Inversion results for the frequency range 0.5–25 Hz (69 logarithmically spaced bins) and distance range 5–125 km (62 bins, 2 km wide each): (a) nonparametric attenuation curves colored by frequency; (b) nonparametric acceleration source spectra colored by magnitude; and (c) site amplification curves for all stations (gray) and reference stations (blue), with the red curve representing the average across reference sites. The color version of this figure is available only in the electronic edition.

GITpy: Application Example

GITpy inversion

To show the potential of GITpy, we present the results of its application to a large dataset collected for Central Italy (CI_db) and described in the Dataset section. As explained earlier, solving the linear system of equation (1) requires constraints to eliminate trade-offs among source, site, and attenuation terms. The first one involves the use of the same six reference stations (LSS, MNF, NRN, SNO, SDM, and SLO) suggested by Lanzano *et al.* (2020) and adopted by Morasca *et al.* (2023). To prevent high-frequency deviations of the source spectra from the ω^2 model, we constrain the site amplification at the reference sites to decay beyond 10 Hz, applying a k-factor of 0.018 s. Furthermore, we assume that the attenuation (in $\log_{10}$ units) at a reference distance of 10 km is 0. This reference distance is selected based on the dataset characteristics, being the smallest distance with a good data distribution (Fig. 1). Figure 3 shows the resulting separated source, attenuation, and site terms produced by GITpy through the module GITeps.py.

GITpy attenuation parameterization

The path attenuation curves show (Fig. 4a) a distance decay of $\sim R^{-2}$ up to 50 km, indicating rapid dissipation of seismic energy near the source. Beyond this distance, ground motion amplifies up to 5 Hz, whereas attenuation steepens at higher frequencies, likely influenced by the Moho discontinuity at ~50 km depth (Agostinetti *et al.*, 2022).

Attenuation is decomposed into geometrical spreading and anelastic attenuation, assuming no exponential source-to-site decay ($\kappa_r = 0$ in equation 13).

The geometrical spreading (Fig. 4b) is estimated by fitting the mean amplitude of nonparametric attenuation curves in the 0.8–1.2 Hz frequency range using a trilinear $G(R)$ model with hinge distances at 40 and 80 km ($n1$ = 1.88, $n2$ = 1.43, and $n3$ = −0.14). The curves are then corrected between 40 and 80 km using both $G(R)$ and an anelastic attenuation model at 1 Hz with $Q_0 = 200$ (Fig. 4c, model T3 in Fig. S2), isolating the remaining attenuation as purely anelastic.

The anelastic attenuation is modeled with a trilinear $Q(f)$ function, capturing high-frequency trends better than a linear model (Fig. 4d). The $Q(f)$ model is characterized by two hinge frequencies ($HF_1 = 0.8$ Hz and $HF_2 = 8$ Hz) defining three distinct slopes for the quality factor. Up to 8 Hz, $Q(f)$ shows two similar increasing trends ($Q_{01} = 242$ and $N_1 = 2.05$; $Q_{02} = 192$ and $N_2 = 0.94$), whereas at higher frequencies ($Q_{03} = 1686$ and $N_3 = -0.11$), $Q(f)$ remains nearly constant.

Residual analysis (Fig. 4e) confirms that FitAttenuation.py effectively models ground-motion attenuation, with a root mean square (rms) residual of 0.02. Although the model slightly underestimates empirical data up to 50 km, especially above 20 Hz, the predicted attenuation curves closely match observed trends.

GITpy source parameterization

The nonparametric source spectra from GITeps.py are fitted using an ω^2 model (equation 2), including an exponential term to account for high-frequency deviations (Bindi and Kotha, 2020). The kappa source (κ_s) is also estimated for each event, representing attenuation effects not captured by the site constraint ($\kappa = 0.018$ s). On average, $\kappa_s \approx 0$, indicating that the assumed κ-value effectively modeled attenuation (Fig. 5a).

For central Italy, a homogeneous model with $V_S = 3.2$ km/s and density = 2.7 g/cm^3 is used. Figure 5a,b shows source parameters, and Figure 5c–f compares modeled and nonparametric spectra. For $M_w > 5.5$, magnitudes are fixed to reference values, from Morasca et al. (2022), based on coda calibration because corner frequencies $f_c < 0.5$ Hz are outside the analyzed range (0.5–25 Hz). An example is the 2016 M_w 6.33 Norcia earthquake, in which fixing M_w was necessary because the spectrum plateau is outside the empirical data frequency range (Fig. 5c).

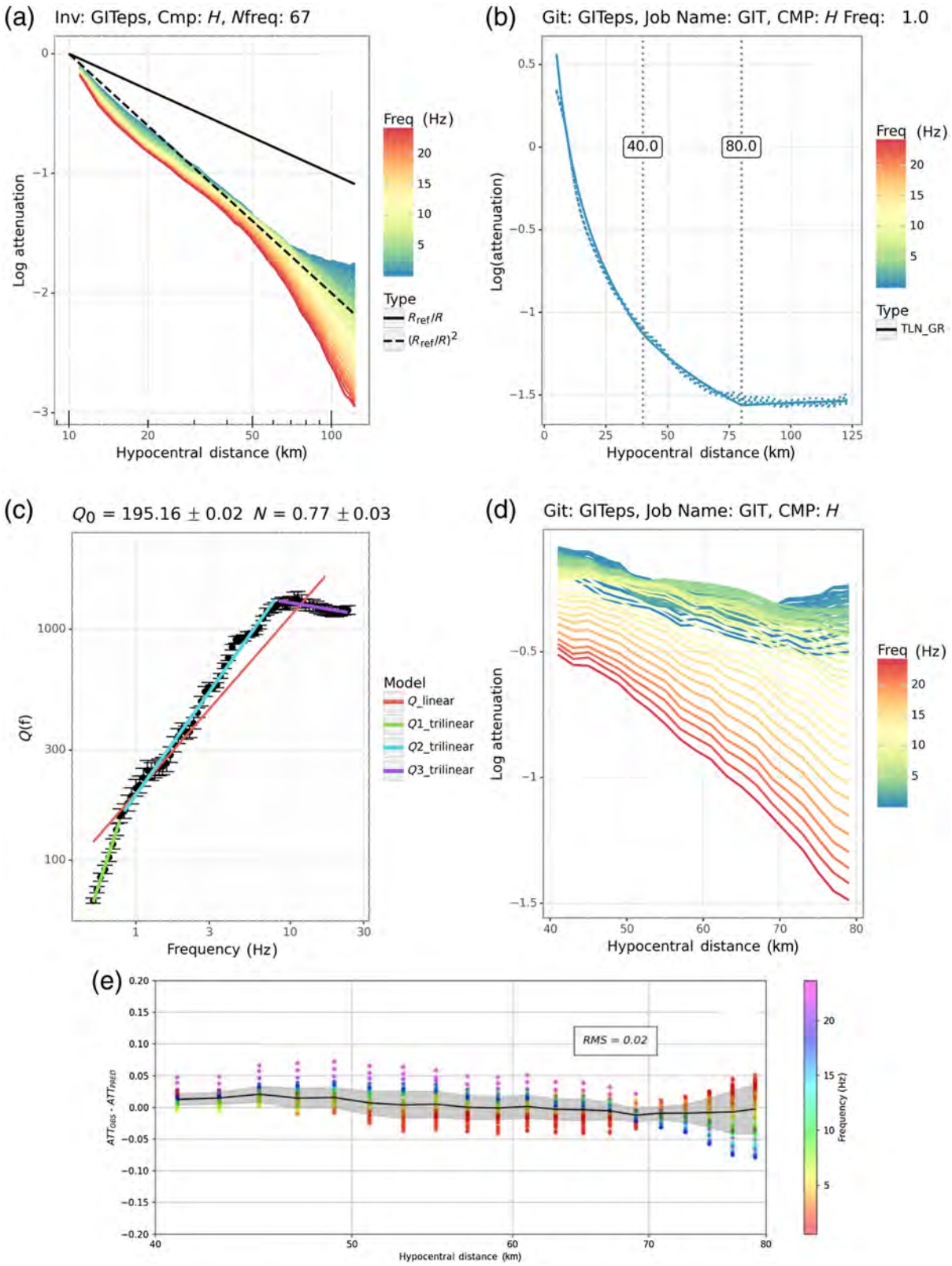

Figure 4. (a) Nonparametric spectral attenuation from CI_db as a function of hypocentral distance; (b) trilinear geometrical spreading $G(R)$ with hinge distances at 40 km (HD1) and 80 km (HD2); (c) nonparametric attenuation corrected for $G(R)$ and anelastic attenuation at 1 Hz; (d) frequency-dependent quality factor $Q(f)$, with the red line showing a linear fit and the red, cyan, and purple lines representing the trilinear model; and (e) residuals between observed and modeled frequency-dependent attenuation as a function of hypocentral distance. The color version of this figure is available only in the electronic edition.

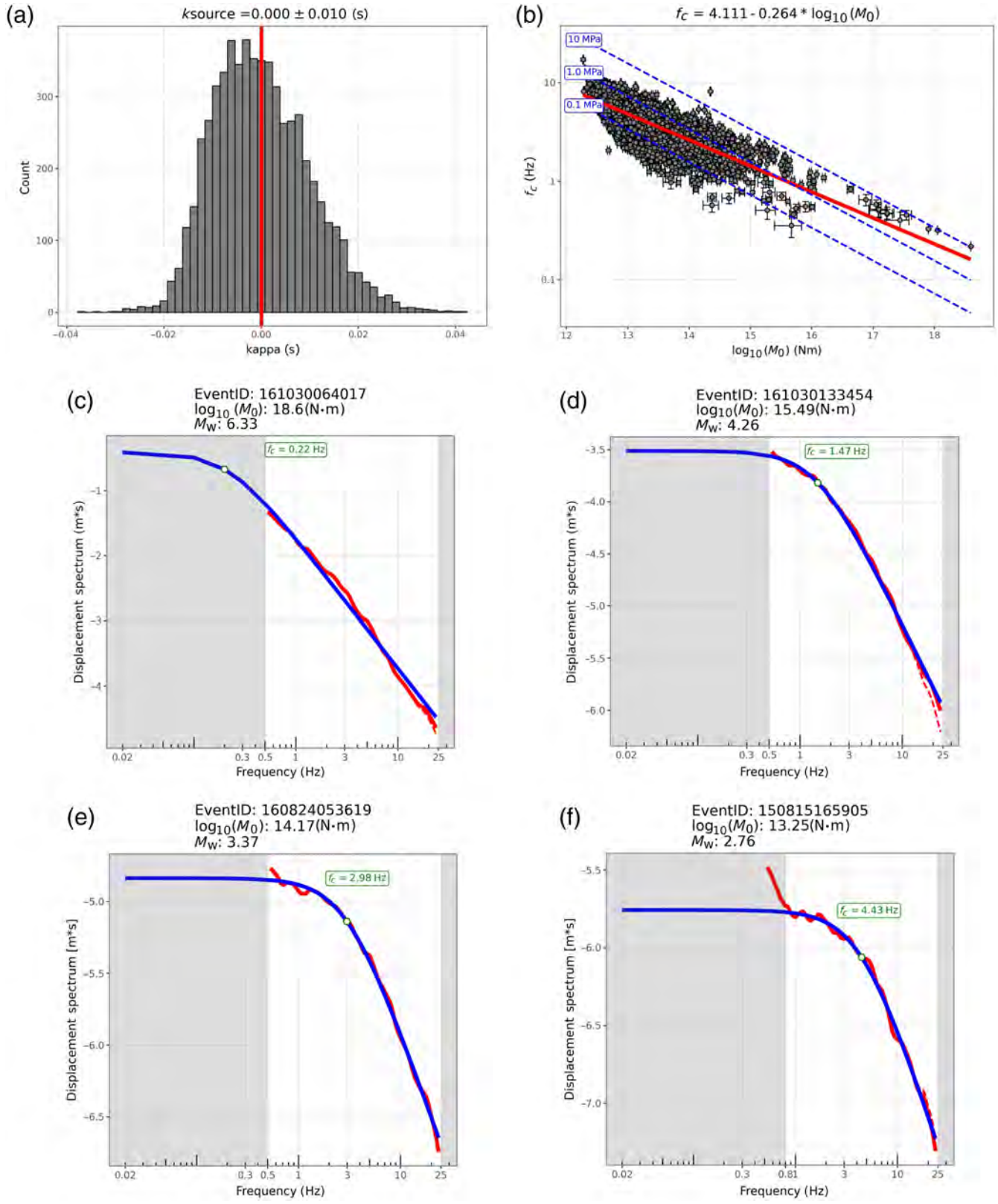

Figure 5. Source spectra modeling: (a) kappa source (κ_s) distribution with the median value; (b) Seismic moment versus corner frequency, with blue dashed lines indicating constant stress drop values; (c) source spectral fitting for the 2016 Norcia event, in which M_w is fixed (Morasca *et al.*, 2022); (d) spectral fitting example for a moderate-magnitude event; and (e) spectral fitting example for a small/moderate-magnitude event. The blue curve represents the Brune model, the red solid curve is the nonparametric spectrum corrected for κ_s, and the red dashed line is the original nonparametric spectrum. The color version of this figure is available only in the electronic edition.

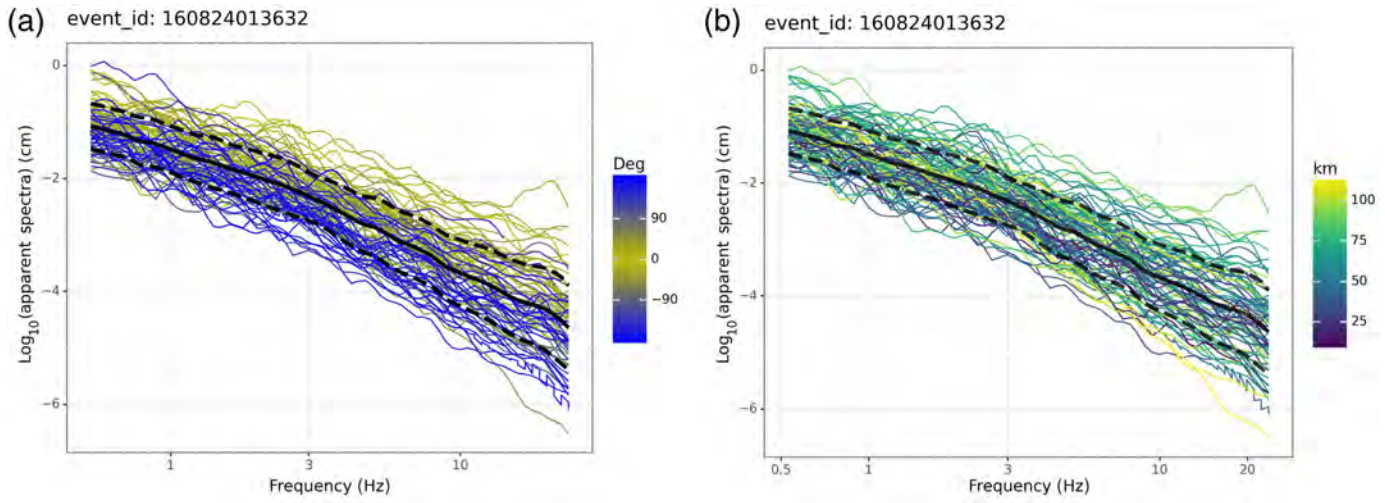

Figure 6. Apparent source spectra for the 24 August 2016 M_w 6 Amatrice mainshock, colored by (a) azimuth and (b) epicentral distance. The black solid line represents the median spectrum, and black dashed lines indicate the standard deviation. The color version of this figure is available only in the electronic edition.

Following recent practice (Bindi and Kotha, 2020; Morasca *et al.*, 2022; Bindi *et al.*, 2024), FitSource.py is used to anchor seismic moments to a reference catalog, ensuring consistency in source parameter interpretation (e.g., stress drop) while maintaining spectral shape. A set of 95 common events with Morasca *et al.* (2022) is used to compute an average source spectra offset (−0.564), with further details in the supplemental material.

GITpy apparent sources

Once the GIT inversion is performed and the three terms (source, attenuation, and site) are separated, empirical models describing these contributions become available for the region. One possibility to push the analysis further is to exploit these pieces of information to calculate apparent source spectra. The CorrectFAS.py module allows correction of the original FAS related to an event of interest for the site and attenuation terms obtained from the inversion, retrieving the source term and parameters as perceived by each station. This is useful for directivity analysis (Colavitti *et al.*, 2022), as shown in Figure 6 for the 24 August 2016 M_w 6 Amatrice event, a well-known case of an event with directivity during the rupture process (Tinti *et al.*, 2016; Calderoni *et al.*, 2017). In addition, CorrectFAS.py enables rapid retrieval of source spectra for new earthquakes in the calibrated region. Without a new inversion, source spectra can be derived by averaging apparent spectra, allowing rapid calculation of source parameters.

Discussion

To validate the equivalence between GITpy and the MATLAB software (Oth *et al.*, 2011) in producing the same inversion outputs, we performed a systematic comparison using identical input data.

Specifically, we compared the GITeps.py module from the GITpy software package with the similar MATLAB-based code by Oth *et al.* (2011) because both implement the same strategy to separate source, attenuation, and site terms using a nonparametric one-step approach. The comparison focused on nonparametric curves, which represent the inversion outputs.

To ensure a direct and fair comparison, we used the same central Italy dataset and applied the same constraints as Morasca *et al.* (2023), which represents our benchmark because the authors also used the MATLAB code from Oth *et al.* (2011).

Consistent with Morasca *et al.* (2023), we selected the same six reference stations (LSS, MNF, SLO, SNO, SDM, and NRN) and assumed a reference distance of 10 km with epicentral distances up to 120 km, divided into 2 km bins. Identical weights were applied for the attenuation constraint at the reference distance, as well as for smoothing conditions on attenuation functions and site conditions.

The comparison of the nonparametric curves obtained from both software packages, using a least-squares inversion, is shown in Figures 7–9. The attenuation curves (Fig. 7) exhibit negligible and distance-independent differences across all frequencies. Similarly, the site and source terms (examples in Figs. 8 and 9) are virtually identical across all frequencies. These results confirm the consistency of both software packages, with variations below 0.05% across the entire dataset for all three terms.

In addition, GITeps.py demonstrated a significantly shorter execution time than the MATLAB software. For instance, performing the inversion at 1 Hz on the same computer (a workstation with a Xeon w7-2475X processor and 256 GB RAM) took only 25 s with GITeps.py, compared to over 2 min with the MATLAB code—an 80% reduction in computation time. Because GIT analysis requires multiple inversions

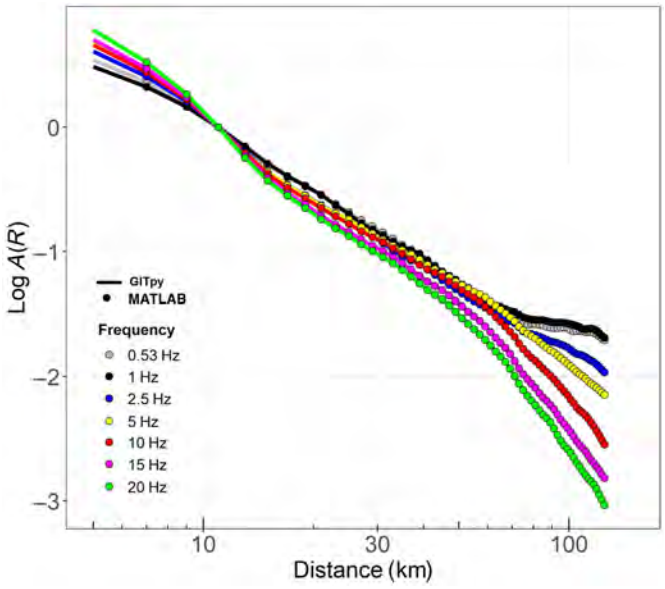

Figure 7. Attenuation comparison between GITpy-derived nonparametric curves (solid lines) and MATLAB code corresponding outputs (circles) for some of the 69 frequencies analyzed in the 0.5–25 Hz range. Each color refers to a different frequency. The color version of this figure is available only in the electronic edition.

(one per frequency in the selected range), this efficiency greatly accelerates the overall analysis process.

Summarizing, these tests demonstrated that the results produced by both Python and MATLAB implementations are numerically consistent, confirming that the Python version accurately replicates the MATLAB outputs. This ensures full reproducibility and supports the reliability of the Python code.

Moreover, by leveraging open-source libraries, the Python implementation enhances accessibility and facilitates integration into broader workflows and application environments. Although both codes achieve the same functional goals, the Python version also benefits from improved maintainability and portability, making it a sustainable alternative for long-term use.

Conclusions

This study introduces GITpy, a Python-based open-source package for GIT applications, using a nonparametric one-step procedure. Available on GitLab (see Data and Resources), its object-oriented structure supports future enhancements.

Although the GIT technique is well known, existing codes are often home-made (Drouet *et al.*, 2008, 2010; Oth *et al.*, 2011), and in some cases, they are available only upon request (Oth *et al.*, 2011). Other open-source alternatives, such as

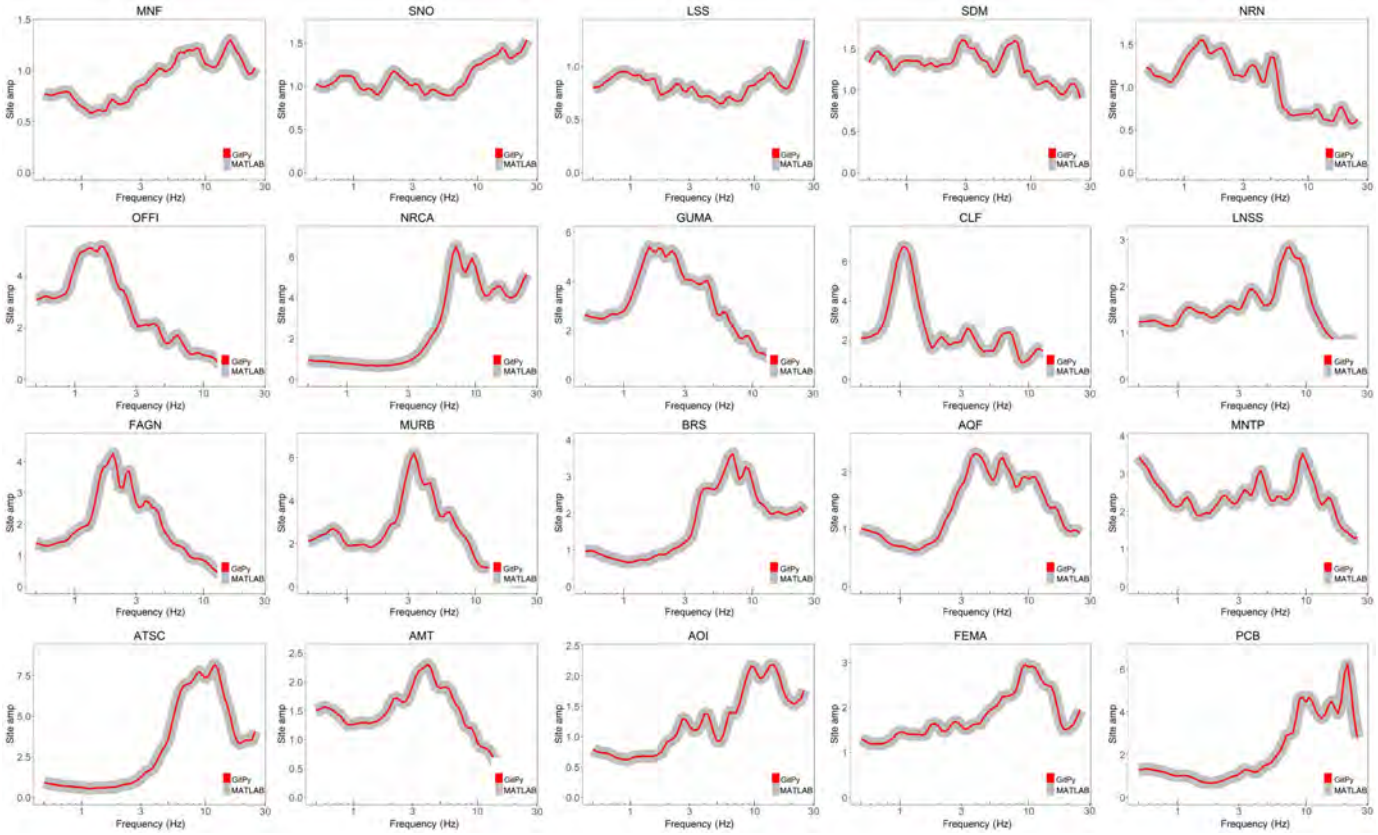

Figure 8. Example of site terms comparison between the GITpy-derived nonparametric curves (red lines) and the MATLAB code corresponding outputs (gray lines). The color version of this figure is available only in the electronic edition.

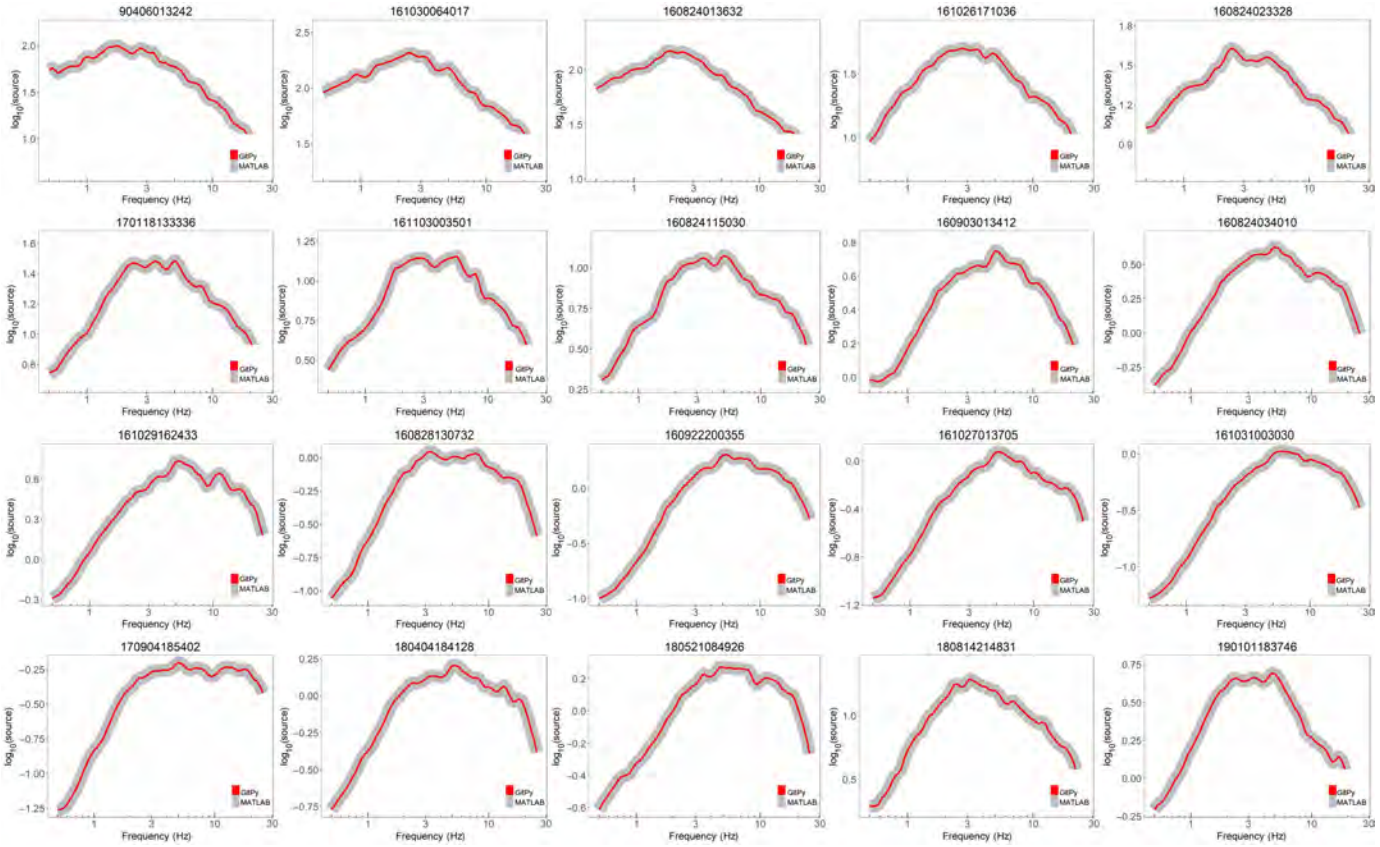

Figure 9. Example of source terms comparison between the GITpy-derived nonparametric curves (red lines) and the MATLAB code corresponding outputs (gray lines). The color version of this figure is available only in the electronic edition.

GITANES (Klin *et al.*, 2018), focus on specific aspects like site amplification, overlooking the modeling of other terms derived from GIT analysis.

The advantage of GITpy lies not only in being an open-source software package that provides a comprehensive analysis of all outputs (including amplification curves, source, and attenuation terms) but also in being Python-based, eliminating the need for a commercial software platform.

GITpy allows users to focus on specific aspects of their analysis depending on the objectives of their study. Regarding attenuation, GITpy provides flexible attenuation modeling with interactive options for testing various models.

Source parameterization follows the ω^2 model (Brune, 1970), estimating numerous source parameters beyond seismic moment and corner frequency. These include stress drop, apparent stress, seismic energy, propagation efficiency, and the ratio of observed to total energy, which evaluates the amount of energy extrapolated outside the frequency range of the data.

The CorrectFAS.py module is a key feature, allowing the calculation of apparent source spectra and source parameters, aiding directivity studies. Furthermore, once calibrated for a region, CorrectFAS.py enables rapid source parameter estimation for new events by correcting FAS using pre-derived attenuation and site functions.

To validate GITpy's efficiency and robustness, we compared its results with those from an alternative MATLAB software (Oth *et al.*, 2011) using the same central Italy dataset (Morasca *et al.*, 2023) and identical constraints. GITpy produced equivalent nonparametric curves while reducing computation time.

GITpy aims to be a reference tool for earthquake source studies, attenuation modeling, and site response analysis. As an open-source resource for geoscientists, it ensures reliable results within efficient time frames. The authors encourage developers to contribute ideas and invite user feedback to enhance the software further.

Data and Resources

The development version of GITpy can be downloaded from the GitLab repository https://gitlab.rm.ingv.it/inversion/gitpy/-/tree/GITpy?ref_type=heads (last accessed January 2025) together with instructions on how to execute the four main modules https://gitlab.rm.ingv.it/inversion/gitpy/-/blob/GITpy/README.md?ref_type=heads (last accessed January 2025) and some examples https://gitlab.rm.ingv.it/inversion/gitpy/-/blob/GITpy/docs/Tutorial.md (last accessed January 2025). A specific version of the GITpy software package can be downloaded at the following link https://gitlab.rm.ingv.it/inversion/gitpy/-/releases (last accessed in September 2024). To find the least-square

solutions of the overdetermined linear system of equations (1), we applied the lsqr method from the SciPy library, specifically designed to solve sparse linear algebra problems; the lsqr Python module can be found at the following link https://docs.scipy.org/doc/scipy/reference/generated/scipy.sparse.linalg.lsqr.html#scipy.sparse.linalg.lsqr (last accessed in September 2024). The authors used data from the National Institute of Geophysics and Volcanology (INGV)-Italian national seismic network (International Federation of Digital Seismograph Networks [FDSN] code IV, doi: 10.13127/SD/X0FXnH7QfY) and from the RAN-Italian strong motion network (FDSN code IT, doi: 10.7914/SN/IT). Referring to the standard of the Standard for the Exchange of Earthquake Data (SEED) format (http://www.fdsn.org/pdf/SEEDManual_V2.4_Appendix-A.pdf, last accessed January 2025). The data and outputs of Morasca *et al.* (2023) used to compare their inversion results with GITpy outputs are available at this link: https://shake.mi.ingv.it/central-italy/ (last accessed January 2025). Part of the analysis to validate GITpy software package were performed using MATLAB software (www.mathworks.com/products/matlab, last accessed January 2025). The supplemental material includes one table and seven figures describing tests for attenuation model calibration, details on source parameterizations, and the validation of the model described in the article.

Declaration of Competing Interests

The authors acknowledge that there are no conflicts of interest recorded.

Acknowledgments

This research is supported by National Institute of Geophysics and Volcanology (INGV) in the frame of the project SECURE (Regional-scale earthquake ground-motion predictions through physics-based and empirical approaches: A case study central Italy), founded by the Italian Ministry of University and Research (MIUR). The authors are sincerely grateful to Editor-in-Chief Allison Bent, reviewer Chuanbin Zhu, and the anonymous reviewer for their valuable and constructive comments, which have significantly improved the quality of this article.

References

Agostinetti, N. P., M. Buttinelli, and C. Chiarabba (2022). Deep structure of the crust in the area of the 2016–2017 Central Italy seismic sequence from receiver function analysis, *Tectonophysics* **826,** 229237, doi:10.1016/j.tecto.2022.229237.

Aki, K., and P. G. Richards (2002). *Quantitative Seismology*, 2nd ed., University Science Books, Sausalito, California, 700 pp.

Ameri, G., A. Oth, M. Pilz, D. Bindi, S. Parolai, L. Luzi, and G. Cultrera (2011). Separation of source and site effects by generalized inversion technique using the aftershock recordings of the 2009 L'Aquila earthquake, *Bull. Earthq. Eng.* **9,** 717–739.

Anderson, J. G., and S. E Hough (1984). A model for the shape of the Fourier amplitude spectrum of acceleration at high frequencies, *Bull. Seismol. Soc. Am.* **74,** no. 5, 1969–1993.

Andrews, D. J. (1986). Objective determination of source parameters and similarity of earthquakes of different size, in *Earthquake Source Mechanics*, S. Das, J. Boatwright, and C. H. Scholz (Editors), Vol. 37, Geophysical Monograph Series, American Geophysical Union, Washington, D.C., 259–267, doi: 10.1029/GM037p0259.

Beeler, N. M., B. Kilgore, A. McGarr, J. Fletcher, J Evans, and S. R. Baker (2012). Observed source parameters for dynamic rupture with non-uniform initial stress and relatively high fracture energy, *J. Struct. Geol.* **38,** 77–89.

Beeler, N. M., T.-F. Wong, and S. H. Hickman (2003). On the expected relationships among apparent stress, static stress drop, effective shear fracture energy, and efficiency, *Bull. Seismol. Soc. Am.* **93,** 1381–1389.

Bindi, D., and S. R. Kotha (2020). Spectral decomposition of the Engineering Strong Motion (ESM) flat file: Regional attenuation, source scaling and Arias stress drop, *Bull. Earthq. Eng.* **18,** 2581–2606, doi: 10.1007/s10518-020-00796-1.

Bindi, D., F. Pacor, L. Luzi, M. Massa, and G. Ameri (2009). The M_w 6.3, 2009 L'Aquila earthquake: Source, path and site effects from spectral analysis of strong motion data, *Geophys. J. Int.* **179,** no. 3, 1573–1579.

Bindi, D., H. N. Razafindrakoto, M. Picozzi, and A. Oth (2021). Stress drop derived from spectral analysis considering the hypocentral depth in the attenuation model: Application to the Ridgecrest region, California, *Bull. Seismol. Soc. Am.* **111,** no. 6, 3175–3188.

Bindi, D., D. Spallarossa, M. Picozzi, and P. Morasca (2020). Reliability of source parameters for small events in central Italy: Insights from spectral decomposition analysis applied to both synthetic and real data, *Bull. Seismol. Soc. Am.* **110,** no. 6, 3139–3157.

Bindi, D., D. Spallarossa, M. Picozzi, A. Oth, P. Morasca, and K. Mayeda (2023a). The community stress-drop validation study—Part I: Source, propagation, and site decomposition of Fourier spectra, *Seismol. Res. Lett.* doi: 10.1785/0220230019.

Bindi, D., D. Spallarossa, M. Picozzi, A. Oth, P. Morasca, and K. Mayeda (2023b). The community stress-drop validation study—Part II: Uncertainties of the source parameters and stress drop analysis, *Seismol. Res. Lett.* doi: 10.1785/0220230020.

Bindi, D., D. Spallarossa, M. Picozzi, and G. Tarchini (2024). Scaling and depth variability of source parameters in central and southern Italy using regional attenuation models, *Bull. Seismol. Soc. Am.* doi: 10.1785/0120240144.

Bindi, D., R. Zaccarelli, F. Cotton, G. Weatherill, and S. R. Kotha (2023). Source scaling and ground-motion variability along the East Anatolian fault, *Seism. Rec.* **3,** no. 4, 311–321, doi: 10.1785/0320230034.

Bindi, D., R. Zaccarelli, H. N. T. Razafindrakoto, M.-H. Yen, and F. Cotton (2023). Empirical shaking scenarios for Europe: A feasibility study, *Geophys. J. Int.* **232,** no. 2, 990–1005, doi: 10.1093/gji/ggac382.

Boatwright, J., J. B. Fletcher, and T. E. Fumal (1991). A general inversion scheme for source, site, and propagation characteristics using multiple recorded sets of moderate-sized earthquakes, *Bull. Seismol. Soc. Am.* **81,** no. 5, 1754–1782.

Brune, J. N. (1970). Tectonic stress and the spectra of seismic shear waves from earthquakes, *J. Geophys. Res.* **75,** 4997–5009.

Brune, J. N. (1971). Correction, *J. Geophys. Res.* **76,** 5002.

Calderoni, G., A. Rovelli, and R. Di Giovambattista (2017). Rupture directivity of the strongest 2016–2017 central Italy earthquakes, *J. Geophys. Res.* **122,** no. 11, 9118–9131.

Castro, R. R., J. G. Anderson, and S. K. Singh (1990). Site response, attenuation and source spectra of *S* waves along the Guerrero, Mexico, subduction zone, *Bull. Seismol. Soc. Am.* **80,** 1481–1503.

Cataldi, L., V. Poggi, G. Costa, S. Parolai, and B. Edwards (2023). Parametric spectral inversion of seismic source, path and site

parameters: Application to northeast Italy, *Geophys. J. Int.* **232,** no. 3, 1926–1943.

Chiaraluce, L., M. Michele, F. Waldhauser, Y. J. Tan, M. Herrmann, D. Spallarossa, G. C. Beroza, M. Cattaneo, C. Chiarabba, P. De Gori, *et al.* (2022). A comprehensive suite of earthquake catalogues for the 2016-2017 Central Italy seismic sequence, *Sci. Data* **9,** 710, doi: 10.1038/s41597-022-01827-z.

Colavitti, L., G. Lanzano, S. Sgobba, F. Pacor, and F. Gallovič (2022). Empirical evidence of frequency-dependent directivity effects from small-to-moderate normal fault earthquakes in central Italy, *J. Geophys. Res.* **127,** no. 6, e2021JB023498 , doi: 10.1029/2021JB023498.

D'Amico, M., P. Morasca, D. Spallarossa, D. Bindi, M. Picozzi, and L. Vitrano (2025). User manual of GITpy: A Python-based tool for the generalized inversion technique, *Rapporti Tecnici INGV*, Vol. 494, 146 pp., doi: 10.13127/rpt/494.

Drouet, S., S. Chevrot, F. Cotton, and A. Souriau (2008). Simultaneous inversion of source spectra, attenuation parameters, and site responses: Application to the data of the French Accelerometric Network, *Bull. Seismol. Soc. Am.* **98,** 198–219.

Drouet, S., F. Cotton, and P. Guéguen (2010). v S30, κ, regional attenuation and Mw from accelerograms: Application to magnitude 3–5 French earthquakes, *Geophys. J. Int.* **182,** 880–898, doi: 10.1111/j.1365-246X.2010.04626.x.

Edwards, B., A. Rietbrock, J. J. Bommer, and B. Baptie (2008). The acquisition of source, path, and site effects from microearthquake recordings using Q tomography: Application to the United Kingdom, *Bull. Seismol. Soc. Am.* **98,** no. 4, doi: 10.1785/0120070127.

Grendas, I., N. Theodoulidis, F. Hollender, and P. Hatzidimitriou (2021). A GIT algorithm for simultaneous estimation of seismic source, site response and regional-distance dependent attenuation parameters: Application to synthetic and real data, *J. Seismol.* **25,** no. 2, 575–598, doi: 10.1007/s10950-020-09975-8.

Ide, S., and G. C. Beroza (2001). Does apparent stress vary with earthquake size? *Geophys. Res. Lett.* **28,** no. 17, 3349–3352, doi: 10.1029/2001GL013106.

Izutani, Y., and H. Kanamori (2001). Scale-dependence of seismic energy-to-moment ratio for strike-slip earthquakes in Japan, *Geophys. Res. Lett.* **28,** 4007–4010, doi: 10.1029/2001GL013402.

Kanamori, H. (1977). The energy release in great earthquakes, *J. Geophys. Res.* **82,** no. 20, 2981–2987.

Klin, P., G. Laurenzano, and E. Priolo (2018). GITANES: A MATLAB package for estimation of site spectral amplification with the generalized inversion technique, *Seismol. Res. Lett.* **89,** no. 1, 182–190, doi: 10.1785/0220170080.

Konno, K., and T. Ohmachi (1998). Ground-motion characteristics estimated from spectral ratio between horizontal and vertical components of microtremor, *Bull. Seismol. Soc. Am.* **88,** no. 1, 228–241, doi: 10.1785/BSSA0880010228.

Lanzano, G., C. Felicetta, F. Pacor, D. Spallarossa, and P. Traversa (2020). Methodology to identify the reference rock sites in regions of medium-to high seismicity: An application in central Italy, *Geophys. J. Int.* **222,** no. 3, 2053–2067.

Morasca, P., D. Bindi, K. Mayeda, J. Roman-Nieves, J. Barno, W. R. Walter, and D. Spallarossa (2022). Source scaling comparison and validation in central Italy: Data intensive direct *s* waves versus the sparse data coda envelope methodology, *Geophys. J. Int.* **231,** no. 3, 1573–1590.

Morasca, P., M. D'Amico, S. Sgobba, G. Lanzano, L. Colavitti, F. Pacor, and D. Spallarossa (2023). Empirical correlations between an FAS non-ergodic ground motion model and a GIT derived model for Central Italy, *Geophys. J. Int.* **233,** no. 1, 51–68, doi: 10.1093/gji/ggac445.

Oth, A., and A. E. Kaiser (2014). Stress release and source scaling of the 2010-2011 Canterbury, New Zealand, earthquake sequence from spectral inversion of ground motion data, *Pure Appl. Geophys.* **171,** no. 10, 2767–2782, doi: 10.1007/s00024-013-0751-1.

Oth, A., S. Parolai, and D. Bindi (2011). Spectral analysis of K-NET and KiK-net data in Japan, Part I: Database compilation and peculiarities, *Bull. Seismol. Soc. Am.* **101,** 652–666.

Pacor, F., F. Gallovič, R. Puglia, L. Luzi, and M. D'Amico (2016). Diminishing high-frequency directivity due to a source effect: Empirical evidence from small earthquakes in the Abruzzo region, Italy, *Geophys. Res. Lett.* **43,** 5000–5008, doi: 10.1002/2016GL068546.

Pacor, F., D. Spallarossa, A. Oth, L. Luzi, R. Puglia, L. Cantore, A. Mercuri, M. D'Amico, and D. Bindi (2016). Spectral models for ground motion prediction in the L'Aquila region (central Italy): Evidence for stress-drop dependence on magnitude and depth, *Geophys. J. Int.* **204,** no. 2, 697–718.

Picozzi, M., D. Bindi, G. Festa, F. Cotton, A. Scala, and N. D'Agostino (2021). Spatiotemporal evolution of microseismicity seismic source properties at the Irpinia near-fault observatory, southern Italy, *Bull. Seismol. Soc. Am.* **112,** 226–242, doi: 10.1785/0120210064.

Savage, J. C., and M. D. Wood (1971). The relation between apparent stress and stress drop, *Bull. Seismol. Soc. Am.* **61,** 1381–1388.

Shible, H., F. Hollender, D. Bindi, P. Traversa, A. Oth, B. Edwards, P. Klin, H. Kawase, I. Grendas, R. R. Castro, *et al.* (2022). GITEC: A generalized inversion technique benchmark, *Bull. Seismol. Soc. Am.* **112,** 850–877, doi: 10.1785/0120210242.

Tinti, E., L. Scognamiglio, A. Michelini, and M. Cocco (2016). Slip heterogeneity and directivity of the M_L 6.0, 2016, Amatrice earthquake estimated with rapid finite-fault inversion, *Geophys. Res. Lett.* **43,** no. 20, 10–745.

Wang, J. H. (2004). The seismic efficiency of the 1999 Chi–Chi, Taiwan, earthquake, *Geophys. Res. Lett.* **31,** L10613 , doi: 10.1029/2004GL019417.

Wang, H., Y. Ren, R. Wen, and P. Xu (2019). Breakdown of earthquake self-similar scaling and source rupture directivity in the 2016–2017 central Italy seismic sequence, *J. Geophys. Res.* **124,** 3898–3917, doi: 10.1029/2018JB016543.

Wyss, M. (1970). Apparent stresses of earthquakes on ridges compared to apparent stresses of earthquakes in trenches, *Geophys. J. Roy. Astron. Soc.* **19,** 479–484, doi: 10.1111/j.1365-246X.1970.tb00153.x.

Zhu, C., S. Bora, B. A. Bradley, and D. Bindi (2024). Spectral decomposition of ground motions in New Zealand using the generalized inversion technique, *Geophys. J. Int.* **238,** no. 1, 364–381, doi: 10.1093/gji/ggae163.

Zollo, A., A. Orefice, and V. Convertito (2014). Source parameter scaling and radiation efficiency of microearthquakes along the Irpinia fault zone in southern Apennines, Italy, *J. Geophys. Res.* **119,** 32563275.

Manuscript received 4 February 2025
Published online 9 July 2025